# Observation of Sub-Poissonian Photon Statistics in a Micromaser

G. Rempe, F. Schmidt-Kaler, and H. Walther
*Sektion Physik der Universität München and Max-Planck-Institut für Quantenoptik, D-8046 Garching bei München, Federal Republich of Germany*
(Received 7 February 1990)

We describe the first investigation of the nonclassical radiation field of a micromaser. The maser cavity is cooled to 0.5 K to exclude thermal photons and has a quality factor of $3\times10^{10}$. Velocity-selected Rydberg atoms pump the maser. The photon statistics in the cavity are measured via the statistics of the atoms leaving the cavity in the lower maser level. Taking into account a detection efficiency of 10%, their fluctuations are reduced up to 40% below the Poisson level. This corresponds to photon-number fluctuations in the cavity of up to 70% below the vacuum-state limit.

PACS numbers: 42.52.+x, 03.65.−w, 32.80.−t, 42.50.Dv

The fact that electromagnetic radiation can show nonclassical properties has recently been widely discussed. There are essentially three phenomena which demonstrate the nonclassical character of light: squeezing (see, for example, Ref. 1), photon antibunching, and sub-Poissonian photon statistics (see, for example, Ref. 2). Methods of nonlinear optics are mostly used to generate nonclassical light, but in special cases such as single-atom resonance fluorescence nonclassical radiation is also obtained.[3] In the following, we describe measurements of the sub-Poissonian photon statistics in a micromaser.[4,5] This setup allows the conditions necessary for obtaining nonclassical radiation to be studied in detail to afford a complete understanding of the generation process.

The micromaser consists of a superconducting microwave cavity with a quality factor as high as $3\times10^{10}$. Rydberg atoms are injected at such a low rate that less than one atom on the average is present inside the resonator at a time. A transition between two neighboring Rydberg levels is resonantly coupled to a single mode of the cavity field. This maser setup has recently been the object of detailed studies, both experimental[4,5] and theoretical.[6-10] It allows one to test many aspects of the interaction between single atoms and a single mode of a quantized field.[11] Rydberg atoms with a very large principal quantum number $n$ are used since the probability of induced transitions between neighboring states scales as $n^4$. In addition, the spontaneous lifetime of the highly excited states is very large. This has the consequence that single photons are sufficient to saturate transitions between adjacent levels. Because of the high quality factor of the cavity the radiation decay time is much larger than the characteristic time of the atom-field interaction, which is given by the reciprocal of the Rabi frequency. It is therefore possible to observe the dynamics of the energy exchange between atom and field mode leading to collapse and revivals in the Rabi oscillations.[5,12] If the mean time interval between atoms injected into the cavity is shorter than the cavity decay time, a field is built up inside the cavity.

The photon statistics of this field are essentially determined by the dimensionless parameter $\Theta=(N_{ex}+1)^{1/2}\Omega t_{int}$, which can be understood as a pump parameter for the micromaser.[6] Here, $N_{ex}$ is the average number of atoms that enter the cavity during the lifetime of the field and $t_{int}$ the time of flight of the atoms through the cavity, which is determined by a velocity selector. For most values of the parameter $\Theta$, the photon statistics turn out to be sub-Poissonian.[6,7] It thus differs from that of standard lasers and masers, which generally show a Poissonian photon-number distribution above threshold.[13]

With the micromaser, the threshold is reached for $\Theta=1$. Here and also at $\Theta=2\pi$ and integer multiples thereof, the photon statistics are super-Poissonian. At these points, the maser field undergoes first-order phase transitions.[6] In the regions between those points sub-Poissonian statistics are expected. The experimental investigation of this behavior is the subject of the following.

The experimental setup is shown in Fig. 1. A highly collimated rubidium atomic beam is used for the maser experiment. The beam of atoms passes through a Fizeau velocity selector. Before entering the superconducting cavity, the atoms are excited into the upper maser level $63^2p_{3/2}$ of $^{85}$Rb by means of the frequency-doubled light of a cw ring dye laser. The laser frequency is stabilized onto the atomic transition $5^2s_{1/2},F=3\rightarrow 63^2p_{3/2}$, which has a width of a few MHz determined by the laser

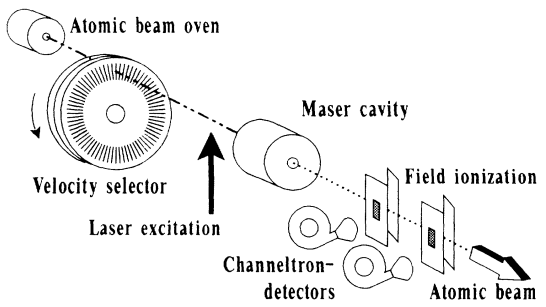


FIG. 1. Scheme of the experimental setup. The Rydberg atoms are excited inside the liquid-$^3$He-cooled environment.

linewidth and transit-time broadening. It is thus possible to prepare a very stable beam of excited atoms. The ultraviolet light is linearly polarized parallel to the electric field of the cavity. Only $\delta m = 0$ transitions are therefore excited by both the laser beam and the microwave field.

The superconducting niobium maser cavity is cooled down to a temperature of 0.5 K by means of a $^3$He cryostat. At this low temperature the number of thermal photons is reduced to about 0.15 at the maser frequency of 21.5 GHz. The cavity quality factor ($3\times10^{10}$) corresponds to a photon storage time of $T_{cav} = 0.2$ s. The cavity is shielded against magnetic fields by several layers of cryoperm. In addition, three pairs of Helmholtz coils are used to compensate the Earth's magnetic field to a value of several mG. This is necessary in order to achieve the high quality factor and to prevent the different magnetic substates of the maser levels from mixing during the atom-field interaction time. Two maser transitions from the $63^2p_{3/2}$ to the $61^2d_{3/2}$ and $61d^2d_{5/2}$ are studied.

The Rydberg atoms in the upper and lower maser levels are detected in two separate field-ionization detectors. The field strength is adjusted so as to ensure that in the first detector the atoms in the upper level are ionized, but not those in the lower level. Atoms in the lower state emitted a photon in the cavity. When those atoms are counted in the second detector, the number of maser photons can be inferred. In addition, the variance of the photon-number distribution can be deduced from the number fluctuations of the lower-level atoms. In the experiment, we are therefore mainly interested in the atoms in the lower maser level.

Experiments are done under steady-state conditions. The number $N$ of atoms in the lower maser level is counted for a fixed time interval $T$ roughly equal to the storage time $T_{cav}$ of the photons. By repeating this measurement many times, the probability distribution $p(N)$ of finding $N$ atoms in the lower level is obtained. The normalized variance[14] $Q_a = [\langle N^2\rangle - \langle N\rangle^2 - \langle N\rangle]/\langle N\rangle$ is evaluated and is used to characterize the deviation from Poissonian statistics. A negative (positive) $Q_a$ value indicates sub-Poissonian (super-Poissonian) statistics, while $Q_a = 0$ corresponds to a Poisson distribution with $\langle N^2\rangle - \langle N\rangle^2 = \langle N\rangle$. The atomic $Q_a$ is related to the normalized variance $Q_f$ of the photon number by

$$Q_a = \epsilon P Q_f (2 + Q_f), \quad (1)$$

which was derived in Ref. 15, with $P$ denoting the probability of finding an atom in the lower maser level. It follows from Eq. (1) that the nonclassical photon statistics can be observed via sub-Poissonian atomic statistics. The detection efficiency $\epsilon$ for the Rydberg atoms reduces the sub-Poissonian character of the experimental result. The detection efficiency was 10% in our experiment; this includes the natural decay of the Rydberg states between the cavity and field ionization. It was determined by both monitoring the power-broadened resonance line as a function of flux[4] and observing the Rabi oscillation for constant flux but different atom-field interaction times.[5] In addition, this result is consistent with all other measurements described in the following especially with those on the second maser phase transition.

Experimental results for the transition $63^2p_{3/2} \leftrightarrow 61^2d_{3/2}$ are shown in Fig. 2. The measured normalized variance $Q_a$ is plotted as a function of the flux of atoms. The atom-field interaction time is fixed at $t_{int} = 50$ $\mu$s. The atom-field coupling constant $\Omega$ (one-photon Rabi frequency) is rather small for this transition, $\Omega = 10$ kHz. A relatively high flux of atoms $N_{ex} > 10$ is therefore needed to drive the micromaser above threshold. The large positive $Q_a$ observed in the experiment proves the large intensity fluctuations at the onset of maser oscillation at $\Theta = 1$. The solid line is plotted according to Eq. (1) using the predictions of the micromaser theory for $Q_f$ or the photon statistics. The error in the signal follows from the statistics of the counting distribution $p(N)$. About $2\times10^4$ measurement intervals are needed to keep the error of $Q_a$ below 1%. The statistics of the atomic beam is measured with a detuned cavity. The result is a Poisson distribution. The error bars of the flux follow from this measurement. The agreement between theory and experiment is good.

The nonclassical photon statistics of the micromaser are observed at a higher flux of atoms or a larger atom-field coupling constant. The $63^2p_{3/2} \leftrightarrow 61^2d_{5/2}$ maser

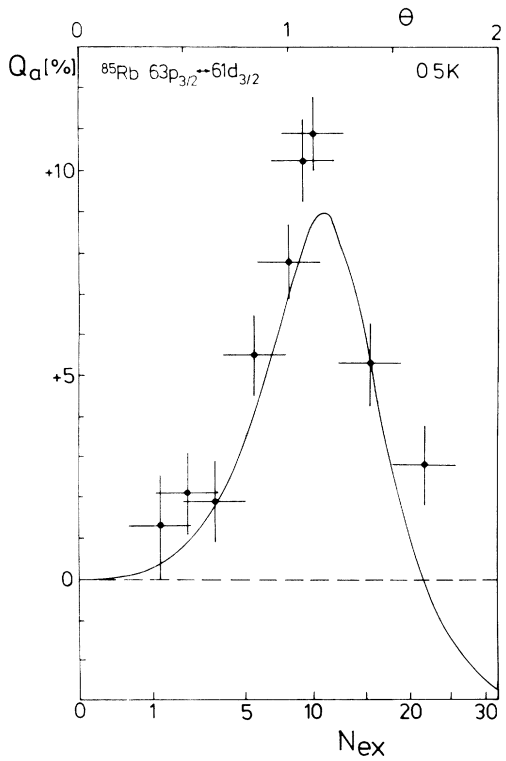


FIG. 2. Variance $Q_a$ of the atoms in the lower maser level as a function of flux $N_{ex}$ near the onset of maser oscillation for the $63^2p_{3/2} \leftrightarrow 61^2d_{3/2}$ transition.

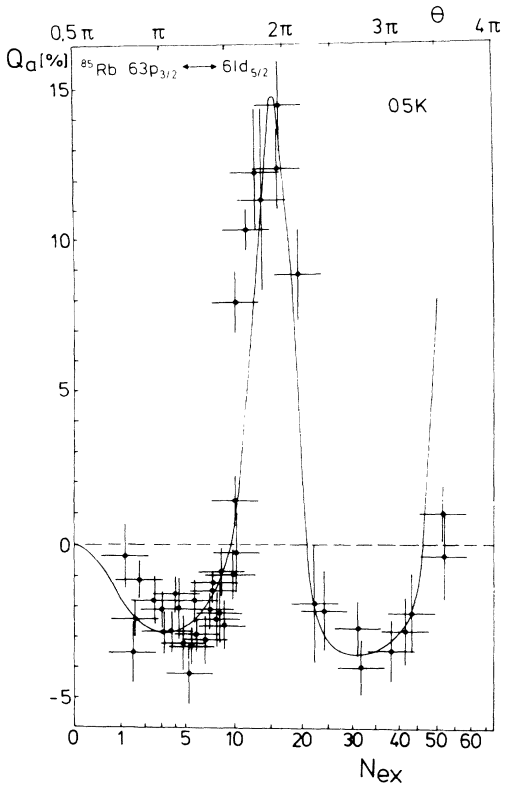


FIG. 3. Same as Fig. 2, but above threshold for the $63^2p_{3/2}\leftrightarrow 61^2d_{5/2}$ transition.

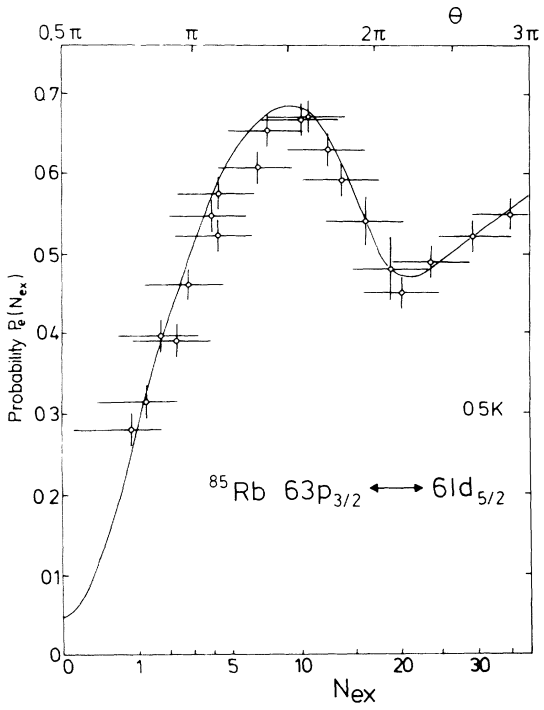


FIG. 4. Probability $P_e(N_{ex})$ of finding the atom in the upper maser level $63p_{3/2}$ for the $63p_{3/2}\leftrightarrow 61d_{5/2}$ transition as a function of the atomic flux.

transition with $\Omega = 44$ kHz is therefore studied. Experimental results are shown in Fig. 3. Fast atoms with an atom-cavity interaction time of $t_{int} = 35$ $\mu$s are used. A very low flux of atoms, $N_{ex} > 1$, is already sufficient to generate a nonclassical maser field. This is the case since the vacuum field initiates a transition of the atom to the lower maser level, thus driving the maser above threshold.

The sub-Poissonian photon statistics can be understood from Fig. 4, where the probability of finding the atom in the upper level is plotted as a function of the atomic flux. The oscillation observed is closely related to the Rabi nutation induced by the maser field. The solid curve was calculated according to the micromaser theory with a velocity dispersion of 4%. A higher flux generally leads to a higher photon number, but for $N_{ex} < 10$ the probability of finding the atom in the lower level decreases. An increase in the photon number is therefore counterbalanced by the fact that the probability of photon emission in the cavity is reduced. This negative feedback leads to stabilization of the photon number.[15]

The feedback changes sign at a flux $N_{ex} \approx 10$, where the second maser phase transition is observed at $\Theta = 2\pi$. This is again characterized by large fluctuations of the photon number. Here, the probability of finding an atom in the lower level increases with increasing flux. For even higher fluxes, the state of the field is again highly nonclassical. The solid line in Fig. 3 represents the result of the micromaser theory using Eq. (1) to calculate $Q_a$. The agreement with the experiment is very good. The sub-Poissonian statistics of atoms near $N_{ex} = 30$, $Q_a = -4\%$ and $P = 0.45$ (see Fig. 4) are generated by a photon field with a variance $\langle n^2\rangle - \langle n\rangle^2 = 0.3\langle n\rangle$, which is 70% below the shot-noise level. Again, this result agrees with the prediction of the theory.[6,7] The mean number

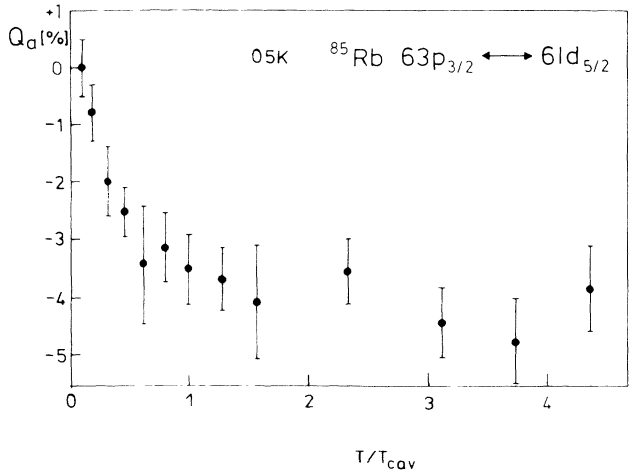


FIG. 5. Variance $Q_a$ of the atoms in the lower maser level as a function of the measurement time interval $T$ for a flux $N_{ex} \approx 30$.

of photons in the cavity is about 2 and 13 in the regions $N_{ex} \approx 3$ and $N_{ex} \approx 30$, respectively. Near $N_{ex} \approx 15$, the photon number changes abruptly between these two values. The next maser phase transition with a super-Poissonian photon-number distribution occurs above $N_{ex} \approx 50$.

Sub-Poissonian statistics are closely related to the phenomenon of antibunching, for which the probability of detecting a next event shows a minimum immediately after a triggering event. The duration of the time interval with reduced probability is of the order of the coherence time of the radiation field. In our case this time is determined by the storage time of the photons. The $Q_a$ value therefore depends on the measuring interval $T$. Experimental results for a flux $N_{ex} \approx 30$ are shown in Fig. 5. The measured $Q_a$ value approaches a time-independent value for $T > T_{cav}$. For very short sampling intervals the statistics of atoms in the lower level show a Poisson distribution. This means that the cavity cannot stabilize the flux of atoms in the lower level on a time scale which is short in relation to the intrinsic cavity damping time.

To summarize, the experimental results presented here clearly show the sub-Poissonian photon statistics of the micromaser field. An increase in the flux of atoms leads to the predicted second maser phase transition. It is interesting that the maser experiment leads to an atomic beam with atoms in the lower maser level showing number fluctuations which are up to 40% below those of a Poissonian distribution found in usual atomic beams. This may lead to interesting new applications, especially in atomic interferometry, which is now being much discussed.

We wish to thank N. Klein for his help in preparing the superconducting cavities.

[1]First demonstration of squeezing: R. E. Slucher, L. W. Hollberg, B. Yurke, J. C. Mertz, and J. F. Valley, Phys. Rev. Lett. **55**, 2409 (1985); for review, see, e.g., H. J. Kimble and D. Walls, J. Opt. Soc. Am. B **4**, 1449 (1987); R. Loudon and P. L. Knight, J. Mod. Opt. **34**, 707 (1987).

[2]First demonstration of photon antibunching: H. J. Kimble, M. Dagenais, and L. Mandel. Phys. Rev. Lett. **39**, 691 (1977). First demonstration of sub-Poissonian photon statistics: R. Short and L. Mandel, Phys. Rev. Lett. **51**, 384 (1983); for review, see, e.g., G. Leuchs, in *Frontiers of Nonequilibrium Statistical Physics,* edited by G. T. Moore and M. O. Scully (Plenum, New York, 1986).

[3]F. Diedrich and H. Walther, Phys. Rev. Lett. **58**, 203 (1987).

[4]D. Meschede, H. Walther, and G. Müller, Phys. Rev. Lett. **54**, 551 (1984).

[5]G. Rempe, H. Walther, and N. Klein, Phys. Rev. Lett. **58**, 353 (1987).

[6]P. Filipowicz, J. Javanainen, and P. Meystre, Phys. Rev. A **34**, 3077 (1986).

[7]L. A. Lugiato, M. O. Scully, and H. Walther, Phys. Rev. A **36**, 740 (1987).

[8]P. Filipowicz, J. Javanainen, and P. Meystre, J. Opt. Soc. Am. B **3**, 906 (1986).

[9]J. Krause, M. O. Scully, and H. Walther, Phys. Rev. A **36**, 4547 (1987).

[10]P. Meystre, G. Rempe, and H. Walther, Opt. Lett. **13**, 1078 (1988).

[11]E. T. Jaynes and F. W. Cummings, Proc. IEEE **51**, 89 (1963).

[12]J. H. Eberly, N. B. Narozhny, and J. J. Sanchez-Mondragon, Phys. Rev. Lett. **44**, 1323 (1980).

[13]Theory is described by, for example, M. Sargent, III, M. O. Scully, and W. E. Lamb, Jr., *Laser Physics* (Addison-Wesley, Reading, MA, 1974); for experiment, see, for example, F. T. Arecchi, Phys. Rev. Lett. **15**, 912 (1965).

[14]L. Mandel, Opt. Lett. **4**, 205 (1979).

[15]G. Rempe and H. Walther, Phys. Rev. A (to be published).

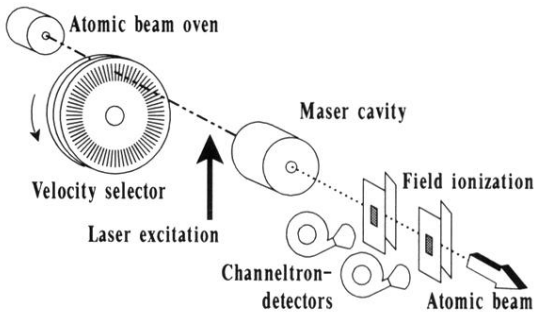


FIG. 1. Scheme of the experimental setup. The Rydberg atoms are excited inside the liquid-$^3$He–cooled environment.